LANDYNE

User Manual

Simulation and Analysis of Kikuchi Patterns

+ SAED Patterns Including Double Diffraction Effect

Table of Contents

Highlight

- A template is provided for creating new crystal structures.
- SAKI can be used for the simulation of Kikuchi lines and SAED patterns with a double diffraction effect.
- A user-friendly index system is for Kikuchi lines and SAED patterns.
- Convert between Miller and Miller-Bravais index.
- Drag and drop action for loading experimental diffraction patterns (.jpg and .tif).
- Align/resize/rotate/invert an experimental SAED/ Kikuchi pattern.
- Compare with the experimental SAED pattern with three Kikuchi pairs (three Kikuchi poles) or two Kikuchi pairs (single Kikuchi pole) to find the precise orientation of the crystal phase.
- Compare with the experimental SAED pattern to reveal the occurrence of forbidden diffraction due to the double diffraction effect.
- Allow saving SAED pattern with Kikuchi lines to .tif, .jpg, .png and .gif formats.
- Prepare figures with labels for publication.
- It provides a periodic table of elements with a molecular mass calculator.
- It provides a table of the number and symbol of the 230 space group.

1. Introduction

Selected area electron diffraction (SAED) analysis has been extensively used in materials science for phase identification, interpretation of twins, coexisting multiple phases, and so forth. The simulation of electron diffraction patterns plays a vital role in interpreting experimental results.

The selected-area mode in a transmission electron microscope can produce three types of electron diffraction patterns, as shown in Table 1.

Table 1. Diffraction patterns in a transmission electron microscope with a parallel incident beam.

	Diffraction pattern	TEM Specimen	Landyne software
(a)	Ring pattern	Polycrystalline specimen	PCED and QPCED
(b)	Spot pattern	Single-crystal region of the specimen	SAED and QSAED
(c)	Kikuchi line pattern		SAKI and SPICA

Diffraction patterns in cases (b) and (c) often occur on the same diffraction pattern. Kikuchi patterns consist of pairs of parallel bright and dark lines. Kikuchi patterns are taken from a single-crystal region of the specimen, which is reasonably thick (~1/2 maximum usable penetration) and has a low defect density.

Kikuchi patterns are significant for the following reasons [Edington, 1975],

(i)   They enable the tasks of obtaining a zone axis of diffraction pattern to be performed more accurately than with spot patterns.

(ii)   They constitute a "Kikuchi map," which describes the distribution of Kikuchi lines within a unit triangle of the stereogram, which can be simulated with Landyne SPICA. The specimen may be tilted in a self-consistent manner while working in the microscope.

(iii)   They determine the sign and magnitude of the deviation s_g from the exact Bragg position. The relationship between the bright Kikuchi line and its associated diffraction spot is used.

(iv)   They define the sense of tilt because the Kikuchi pattern behaves as if it is fixed to the crystal's bottom. Consequently, it moves in the same sense as the crystal; that is, the lines move in a direction perpendicular to the tilt axis and towards the edge of the specimen tilted up.

(v)   Small angular tilts, δ, can be estimated, where $\delta = m/L$ and m is the linear displacement of the Kikuchi line pattern, normal to the tilt axis; L is the camera length.

(vi)   Large angular tilts can be measured by identifying specific $\mathbf{B} = \mathbf{g_1}\char`^\mathbf{g_2}$ accurately.

(vii)   They determine crystal symmetry because, unlike spot patterns, Kikuchi patterns exhibit real crystal symmetry.

SAKI is designed for the simulation and analysis of Kikuchi patterns and SAED with a double diffraction effect. The current version is 5x. It is one of the key computer programs in the Landyne suite for electron diffraction simulation and crystallographic analysis.

2. Theory background

When the TEM sample is reasonably thick but is still transparent primarily to electrons, incoherent scattering contributes a diffuse background to the diffraction pattern. More interesting, intersecting sets of straight lines appear on top of this diffuse background. These are Kikuchi lines, which may be either bright or dark but are impressively straight and regularly arranged. They provide crucial crystallographic information about the sample. Kikuchi lines can be more pronounced in CBED patterns than in SAED patterns because: i) CBED patterns arise from a smaller and thus more uniform region than SAED patterns; and ii) The enhancement of coherent and elastic scattering in CBED.

The main features of the geometry of Kikuchi patterns can be understood by using the simplified treatment, which was first proposed by Kikuchi in 1928: the lines arise from the diffraction of electrons that have been previously inelastically scattered by a specimen. These inelastically scattered electrons are present in SAED patterns, both as a diffuse halo around the transmitted and strong diffracted spots as overall faint background intensities. Since many more electrons suffer small energy changes than large ones, the diffuse halo loses intensity with increasing distance from the transmitted beam. The intensity distribution may be described in terms of the polar diagram in Figure 1.

2.1 Simulation of Kikuchi pattern

Kikuchi lines are useful for the precise determination of the specimen orientation in TEM experiments. The location of the Kikuchi line is related to the sign and magnitude of the deviation parameter, s_g of the diffraction spot with a vector of g,

$$x = \frac{sR}{g^2\lambda}$$

where x is the distance from the diffraction spot at R to its corresponding bright Kikuchi line; λ is the incident electron beam's wavelength.
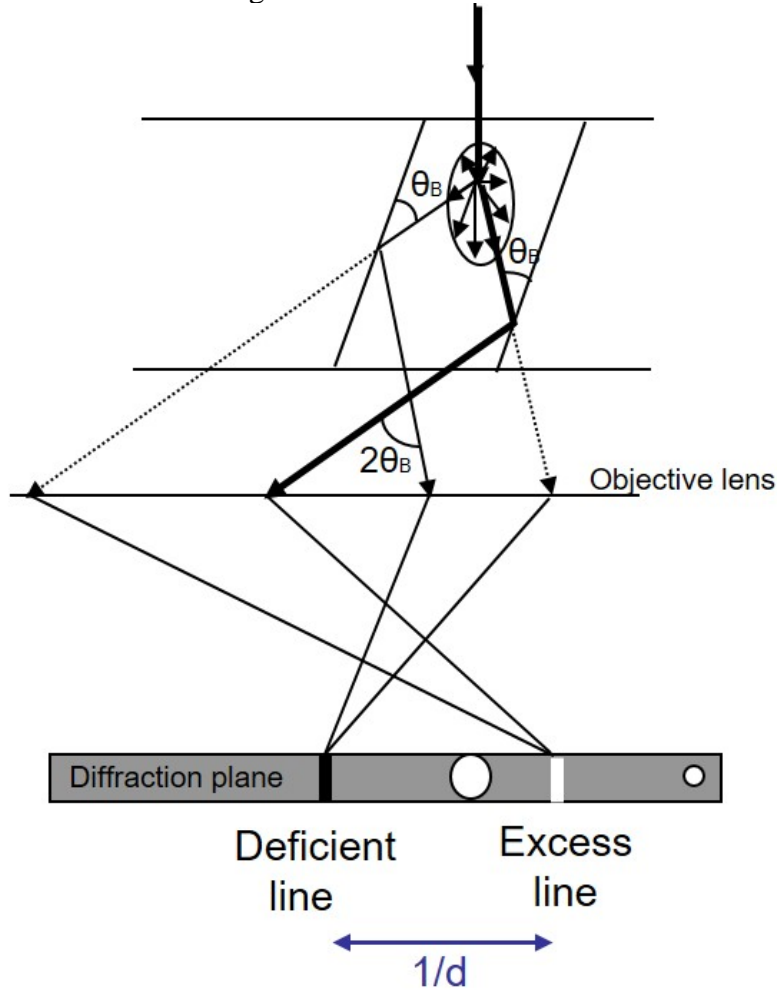

Figure 1. The geometry of Kikuchi lines in electron diffraction of a single crystal.

2.2 The determination of the precise orientation from three Kikuchi bands

The analysis for the crystal orientation unambiguously requires three nonparallel Kikuchi line pairs in a SAED pattern. The direction of the incident electron beam (OO') is specified in the angles to the zone axes of the Kikuchi poles (A, B, and C) in Figure 2,

$$\phi \approx R/L$$

Where R is the distance of OA, OB, and OC, while L is the camera length.

Due to the inward curvature of the Ewald sphere, indices, and zone axes satisfy,
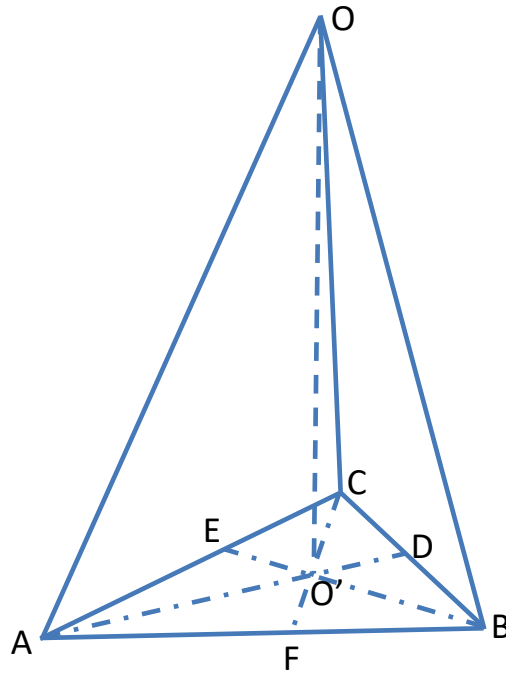
$$(hkl) * [uvw] > 0$$

Figure 2. The incident beam (OO') and Kikuchi poles (OA, OB, OC) are related.

Here, the (h k l) refers to the outer line of each Kikuchi pair, and the [u v w] refers to the other Kikuchi pole, which is on the side of the Kikuchi pair. SAKI provides a step-by-step approach to analyze the precise orientation from a set of three Kikuchi line pairs in a SAED pattern.

The precise orientation of the crystal can be derived from the incident electron beam positions and three Kikuchi poles. SAKI analysis can be applied to all seven crystal systems.

Method 1. Analytical equations

$$\cos(\Phi_i) = \frac{\boldsymbol{u_i} \cdot \boldsymbol{r}}{|\boldsymbol{u_i}||\boldsymbol{r}|}$$

Let's assume $|\boldsymbol{r}| = 1$, three linear equations can be solved, $\boldsymbol{r}$ = [u, v, w].

Method 2. Vector analysis

$$f_1 = \frac{1}{cos\varphi_1} = \sqrt{1 + (\frac{AO'}{OO'})^2}$$

$$f_2 = \frac{1}{cos\varphi_2} = \sqrt{1 + (\frac{BO'}{OO'})^2}$$

$$f_3 = \frac{1}{cos\varphi_3} = \sqrt{1 + (\frac{CO'}{OO'})^2}$$

$$\overrightarrow{OA} = f_1 \frac{OO'}{|u_1 v_1 w_1|} [u_1 v_1 w_1]$$
$$\overrightarrow{OB} = f_2 \frac{OO'}{|u_2 v_2 w_2|} [u_2 v_2 w_2]$$
$$\overrightarrow{OC} = f_3 \frac{OO'}{|u_3 v_3 w_3|} [u_3 v_3 w_3]$$

$$[uvw] = \overrightarrow{OO'} = \frac{O'D}{AD} \overrightarrow{OA} + \frac{O'E}{BE} \overrightarrow{OB} + \frac{O'F}{CF} \overrightarrow{OC}$$

We notice the relation, $\qquad 1 = \frac{O'D}{AD} + \frac{O'E}{BE} + \frac{O'F}{CF}$.

2.3 The determination of the precise orientation from two Kikuchi bands

Here, we adopted the ODS method by Otte, Dash and Schaak (1964) and the HF-K method by Helfmeier and Feller-Kniepmeer (1977) for the orientation along the primary beam from two independent Kikuchi pairs (or a single Kikuchi pole).

In the two methods, it is assumed that the Kikuchi pairs were indexed, and the positions of the incident beam and the Kikuchi pairs were located.
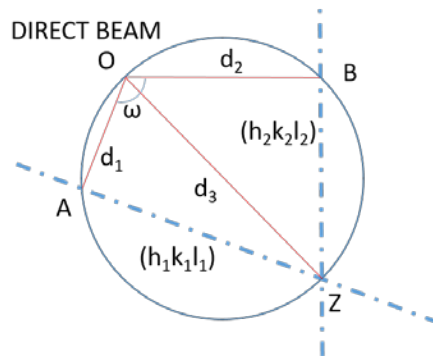

Figure 3. The traces of the diffracting planes, $(h_1 k_1 l_1)$ and $(h_2 k_2 l_2)$. The symbols used in describing the orientation determination from the Kikuchi pattern.

We introduced the ODS method first. As shown in Figure 3, two traces, AZ and BZ, from planes (h1k1l1) and (h2k2l2), respectively, are drawn intersecting at Z, which is the zone axis. Now, the points OAZB lie in a circle, so it follows that

$$OI = d_3 = (d_1^2 + d_2^2 - 2\,d_1 d_2\,cos\omega)^{1/2}/sin\omega \qquad (1)$$

where d_1, d_2, and ω are the distances OA, OB, and the angle <AOB, respectively. The diagram has been redrawn and relabeled to make the two methods easier to compare. A typo in the formula [1] in the original paper has been corrected.

If the effective camera length is L, the distances d_1, d_2, and d_3 correspond to the small angles (less than 5° in general, since L >> d) $sin\chi_1 \approx \chi_1 = d_1/L$, $sin\chi_2 \approx \chi_2 = d_2/L$, $sin\chi_3 \approx \chi_3 = d_3/L$. Respectively, these are the angles between the directions OA and $\hat{\boldsymbol{p}} = [h_1 k_1 l_1]$, OB and $\hat{\boldsymbol{q}} = [h_2 k_2 l_2]$, $\hat{\boldsymbol{k}}$ and $\pm\,(\hat{\boldsymbol{p}} \times \hat{\boldsymbol{q}})\,\|\,\hat{\boldsymbol{r}} = [h_3 k_3 l_3]$ where $\hat{\boldsymbol{k}}$ is the normal to the plane of the diffraction pattern. $\hat{\boldsymbol{p}}, \hat{\boldsymbol{q}}, \hat{\boldsymbol{r}}$ and $\hat{\boldsymbol{k}}$ are all unit vectors.

We have that

$$\hat{\boldsymbol{k}} = e_1\hat{\boldsymbol{p}} + e_2\hat{\boldsymbol{q}} + e_3\hat{\boldsymbol{r}} \qquad (2)$$

where

$$e_1 = \frac{sin\chi_1 - sin\chi_2 cos\delta}{sin^2\delta}, \qquad (3)$$

$$e_2 = \frac{sin\chi_2 - sin\chi_1 cos\delta}{sin^2\delta}, \qquad (4)$$

$$e_3 = (sin^2\delta - sin^2\chi_1 - sin^2\chi_2 + 2cos\delta sin\chi_1 sin\chi_2)^{1/2}/sin\delta, \qquad (5)$$

$$cos\delta = \hat{\boldsymbol{p}} \cdot \hat{\boldsymbol{q}}, \; sin\delta = |\hat{\boldsymbol{p}} \times \hat{\boldsymbol{q}}| \qquad (6)$$

The HF-K method: The solution is derived from a tripod of $\boldsymbol{g}_1, \boldsymbol{g}_2$, and $\boldsymbol{Z} = \boldsymbol{g}_1 \times \boldsymbol{g}_2$. To compare the ODS method, we reassign $\hat{\boldsymbol{p}} = \frac{\boldsymbol{g}_1}{|\boldsymbol{g}_1|}, \hat{\boldsymbol{q}} = \frac{\boldsymbol{g}_2}{|\boldsymbol{g}_2|}$ and $\hat{\boldsymbol{r}} = \frac{\boldsymbol{Z}}{|\boldsymbol{Z}|}$. The proper negative beam direction $\hat{\boldsymbol{k}}$ is therefore given by

$$\hat{\boldsymbol{k}} = \hat{\boldsymbol{r}} - L_1 f_1 \hat{\boldsymbol{p}} - L_2 f_2 \hat{\boldsymbol{q}} \qquad (7)$$

where L_1 and L_2 are the sides of the parallelogram in Fig. 4, and the f_i (i = 1, 2) is the factor converting measured distances into angles. The diagram has been redrawn and relabeled to make the two methods easier to compare. The only data to be measured from the pattern are the spacings of the two Kikuchi pairs, b_1 and b_2, and the angle (ω) between them. The analytical solutions for L_1 and L_2 are

$$L_1 = \frac{d_1 - d_2 cos\omega}{sin^2\omega} \qquad (8)$$

$$L_2 = \frac{d_2 - d_1 cos\omega}{sin^2\omega} \qquad (9)$$

The conversion factor can be calculated to be

$$f_i = tan\left[2\,arcsin\left(\frac{g_i}{2k}\right)\right]/b_i, \qquad (10)$$

Here g_i is the length of a reciprocal lattice vector, k equals $1/\lambda$, and λ is the wavelength.
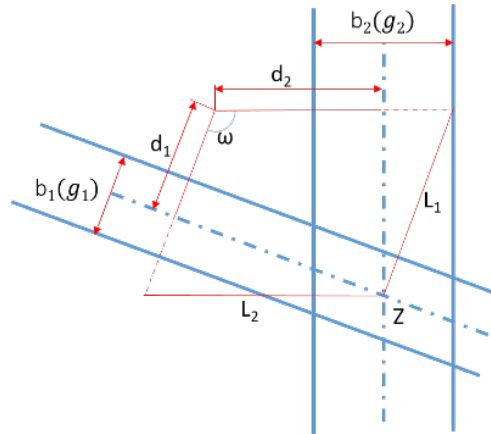

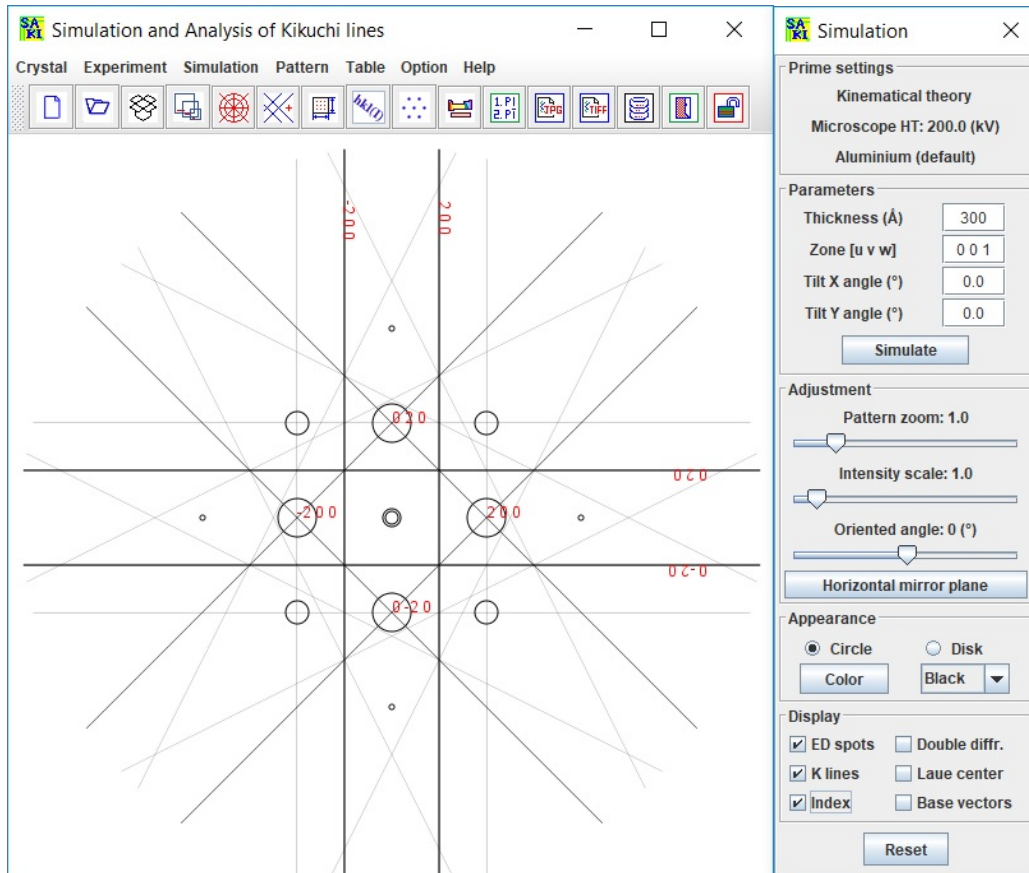Figure 4. Schematic diagram demonstrating analysis of Kikuchi line pairs.

Figure 5. A snapshot of the main panels in SAKI with a simulated Kikuchi pattern of Al [001].

2.4 Kikuchi map

Kikuchi maps consist of a montage of Kikuchi patterns taken with different incident electron beams positioned in the stereogram's unit triangle's corresponding place. All the Kikuchi lines join up to produce a 'road' map of the unit triangle. The simulation of Kikuchi is given in SPICA software.

2.5 Double diffraction effect

When a TEM specimen is thin enough, only single scatterings need to be considered to interpret the experimental results. Otherwise, multiple beam dynamical scatterings should be used for the analysis of the experimental results. Double diffraction is a simplified model where an electron diffracts twice before leaving the specimen. It requires that the electron beam from the first diffraction serve as the incident beam for the second diffraction. Most TEM samples are sufficiently thick that electrons can undergo multiple diffractions, especially when s ≈ 0. A dynamical theory is unavoidable for calculation in detail. However, some aspects of multiple diffractions can be understood by straightforward geometrical considerations and the kinematical theory - for example, the occurrence of forbidden diffraction spots and interactions between two crystallites. SAKI deals with the first case. The central idea is that a diffracted electron acts as an incident beam for the second diffraction.
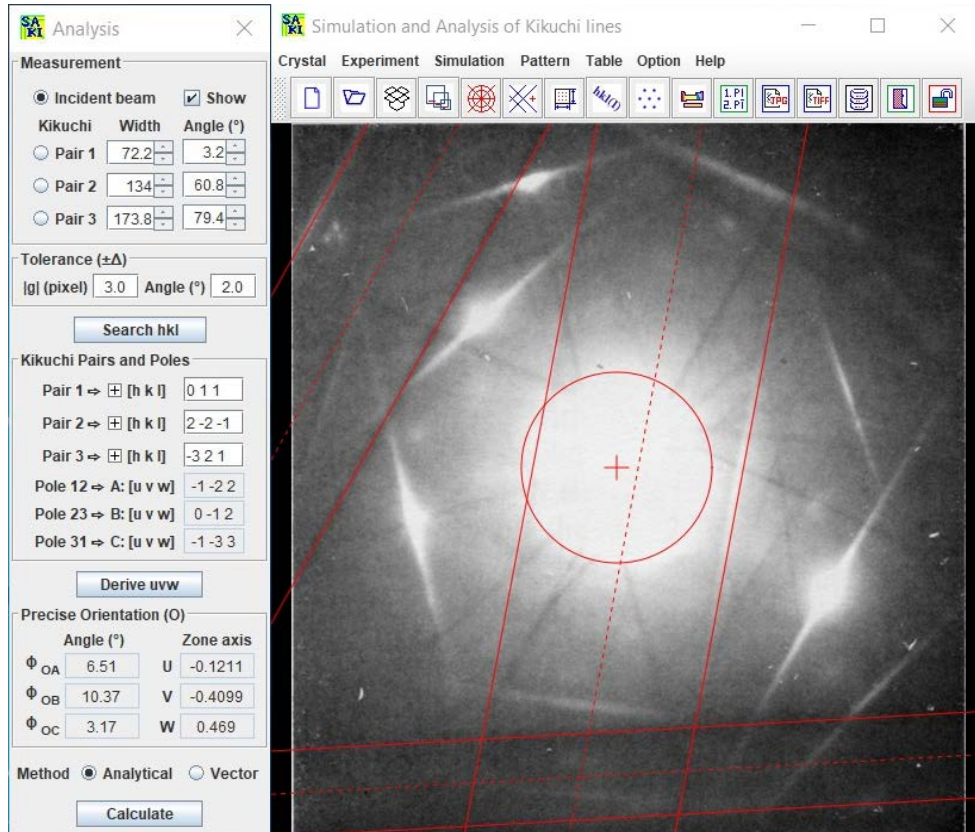

Figure 6. A snapshot of the main panels in SAKI, including a Kikuchi pattern of Mg.

3. The graphic user interface of SAKI

3.1 Main interface

The main interface of SAKI is a frame with a menu, a toolbar, and a calculation dialogue panel, as shown in Figure 5. The frame of SAKI with an experimental SAED pattern and an analysis dialogue panel is shown in Figure 6. The menu gives more text descriptions and is organized in groups, while the toolbar shows graphics and easy access. Most functions of the menu and the toolbar are the same; some functions are only provided in the toolbar.

3.2 Tools and options

Besides the main interface shown above, various tools and options are available to assist in the simulation and analysis process. A new crystal data file can be prepared with a template, as shown in Figure 7. Experimental diffraction patterns can be processed for resizing, rotation, and alignment. The precise orientation can be expressed in angles and rational indices of the Azone axis. The indices of spots and Kikuchi patterns can be displayed using intensity as a threshold. Miller index and Miller-Bravais index can be converted into each other. The output area can be set up and saved as in .jpg or .tif format. A periodic table of elements and a list of the space groups are provided.
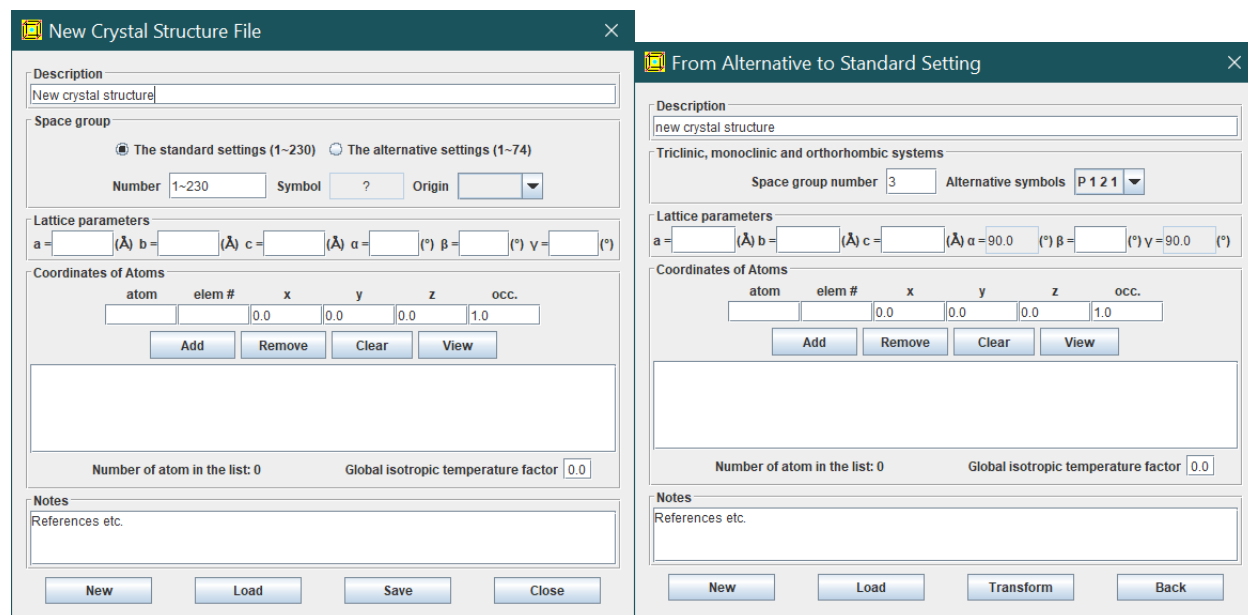

Figure 7. A snapshot of the crystal data templates, standard, and alternative settings.

4. Usage of SAKI

SAKI is mainly coded in Java and partially coded for PC with Microsoft Windows only. Thus, the Landyne suite requires Java Runtime Environment above JRE 1.8.0. The SAKI is one key component in the Landyne software suite, which can be downloaded from the Landyne website:

Decompress the installation file landyne5.z7 in a selected directory and execute landyne.exe by double clicking. SAKI usage is straightforward: firstly, to load structure data and set up input parameters, then click the **Simulate** button in the **Simulation** control panel.

The necessary steps for using SAKI are listed here,

i)   The toolbar displays the most frequently used functions, which can be hidden for a small monitor.

ii)   A new crystal data file can be created using the template.

iii)   A crystal data file can be loaded in the menu file system.

iv)   Experimental diffraction patterns in JPEG or TIFF format can be loaded in the menu file system or directly by drag and drop using the mouse.

v)   The precise orientation can be derived using three Kikuchi poles in the experimental diffraction pattern. Two methods, analytical equations, and the vector analysis, are available.

vi)   Click the simulate button in the simulation dialogue panel to create a diffraction spot and Kikuchi pattern, make resizing and rotation adjustments, choose the appearance, and other display options.

vii)   Spot patterns and Kikuchi lines can be indexed separately.

viii)   Miller and Miller-Bravais index can be converted with a hexagonal system dialogue panel.

ix)   The final result can be saved as an image in the format of JPEG or TIFF.

4. 1 Prepare new data file

A structure data file can be prepared using the **New Crystal Structure File** dialogue window in Figure 7. The dialogue window provides an automatic assistant for the user and makes sure to meet the requirements of the file format. The template is embedded with the 230 space groups in the Hermann-Mauguin notation, which is listed in the International Table for Crystallography. However, only b unique axis will be used in a monoclinic system. Two origin choices can be accepted as input parameters, but choice 2 will be converted to choice 1. To save the data structure, click the **Save** button, or make a new one, click the **New** button.

The crystal file can also be converted from previous data for modification or from a crystallographic information file (CIF). If a data file in an alternative setting of space group for triclinic, monoclinic, and orthorhombic systems is used, please click on the alternative settings (1~74). A tool for the transformation of files in the nonconventional notations to the standard notations is provided.

4.2 Simulation

Kinematical diffraction theory is used in the simulation. Basic parameters for simulation, e.g., high voltage, pattern zoom, and intensity scale, can be adjusted in the **Simulation** menu.

After structure data for simulation is loaded and the setup of thickness, zone axis, and tilt angles, a new diffraction pattern is generated by clicking the **Simulate** button. The pattern can be adjusted by changing other parameters.
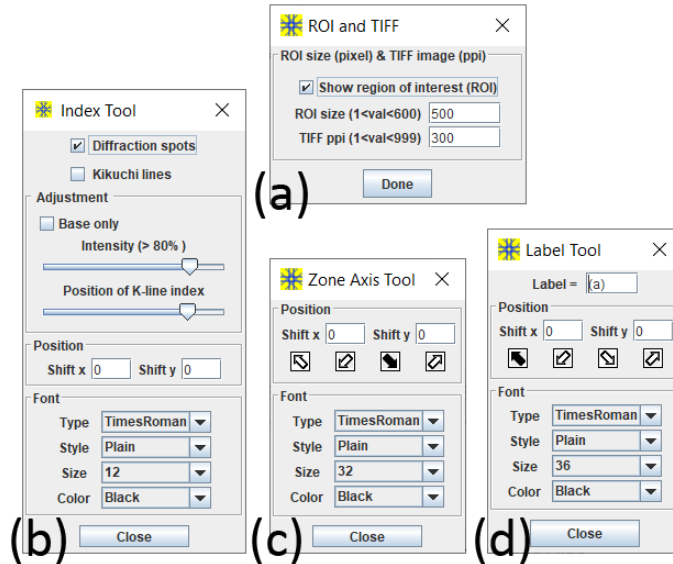

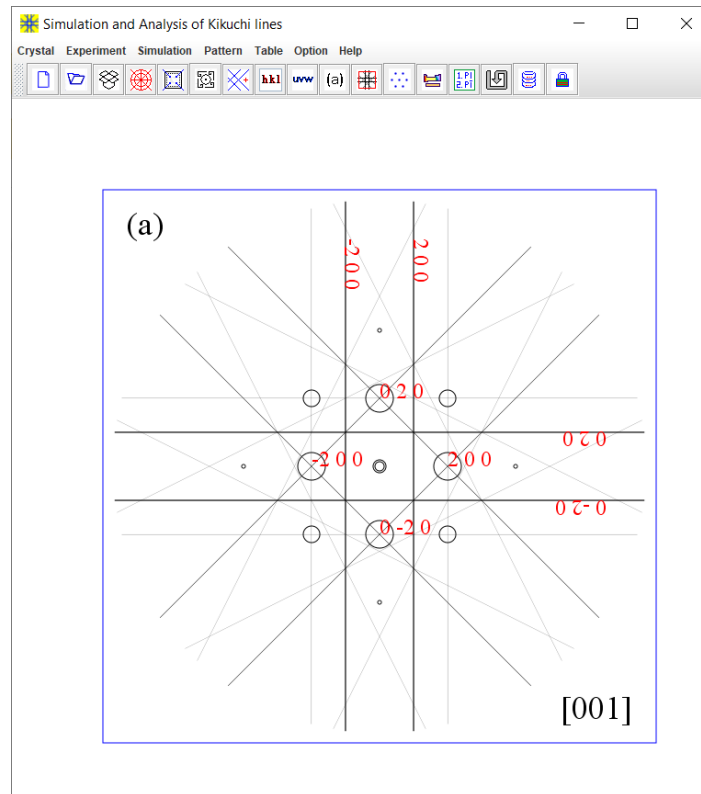Figure 8. A snapshot of the tools for labeling a simulated pattern.

Figure 9. A snapshot of a simulated pattern with labels.

Orientation and mirror operation are used to orient the simulated pattern to match the experimental pattern and generate various twins.

Diffraction patterns can be viewed in open or solid circles and various colors. A kinematical or double diffraction pattern can be displayed. The index can be labeled for basic reciprocal vectors and diffraction spots selected by the intensity level. Basic vectors and Laue center can be displayed and hidden.

4.3 Sava figures for publication

Together with experimental images, these simulated patterns can be saved to images that are ready for publication. Figure 8 shows the tools of (a) region of interest, (b) index, (c) zone axis, and (d) figure label. Figure 9. shows a simulated image within a region ready for saving in .tif, .jpg, .png, or .gif formats.

4.4 Load an experimental image

An experimental diffraction pattern can be loaded through the MS-Window file system or by drag and drop operation. Figure 10 shows the three operations on the images. For alignment, let us select a selected point on an image with the mouse pointer, and right-click will bring the selected point to the center of the screen. The resize and rotation operations will change the image but keep the selected point unchanged. A new alignment can be done on the resized and rotated image.

4.5 Operation steps for analysis

SAKI [Li, 2020a] can be used to determine the index and the zone axis of an experimental diffraction pattern and precise orientation using three Kikuchi poles if it belongs to a known crystal structure. Figure 6 shows the analysis dialogue panel.
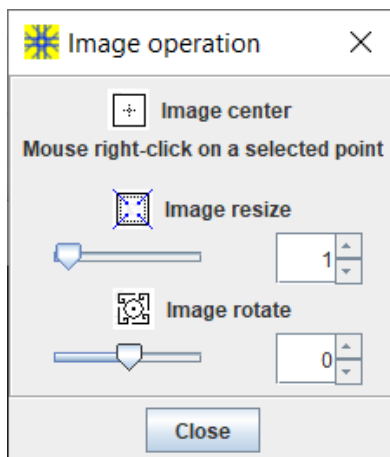

Figure 10. A snapshot of image operation for alignment, resize, and rotation.
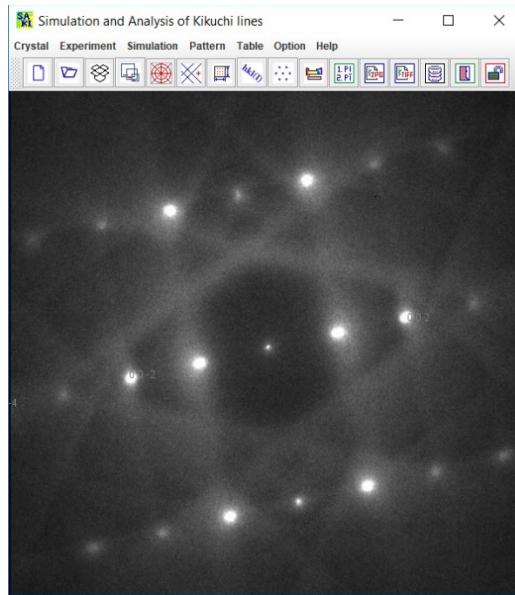
Figure 11. Experimental SAED pattern of the Cr_3Ge phase in the display panel of the SAKI. The zone axis was determined to be [210].
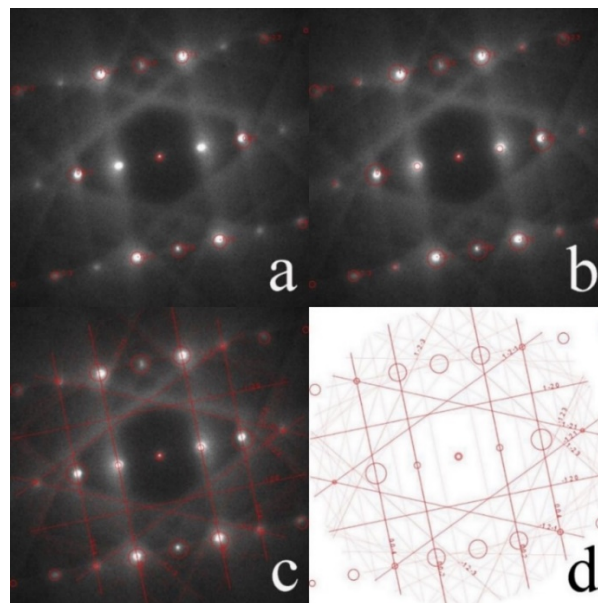

Figure 12. (a) Simulated spot pattern in kinematical diffraction, (b) with a double diffraction effect. (c) Simulated Kikuchi pattern supposed on the experimental pattern (d) the simulated pattern only for clarity.

Step 1. Set up an R-spacing marker using the scale bar on the experimental pattern. **Adjust** the calibration circle using the pattern zoom and then lock it down.
Step 2. In the analysis dialogue panel, choose incident beam (default) or Kikuchi pair1, pair2, pair3, and check the show box. Adjust the width, the orientation, and the position with the mouse.
Step 3. Define the tolerance value for width (default 3 pixels) and angle (2°), save possible indices to a file, and then search the suitable index.

Step 4. The zone axes are generated with the input indices of the Kikuchi pairs.

Step 5. The precise orientation can be expressed in the angles to the Kikuchi poles or the zone axis in rational numbers. The Miller-Bravais index for a hexagonal system can be converted with the optional tool.

Step 6. Double diffraction effects on SAED diffraction patterns can be added by simply selecting the option.

5. Application examples

Kikuchi analysis has various applications, as listed in the introduction part. Application examples are given in the following.

5.1 Simulation of spot and Kikuchi diffraction patterns

The Cr_3Ge phase was found in CoFeCrGe Heusler alloy [Jin, Li, Sellmyer 2018]. Figure 11 shows the experimental diffraction pattern of the Cr_3Ge phase. The zone axis was determined to be [210]. Figure 12 shows (a) a simulated spot pattern in kinematical diffraction, (b) with a double diffraction effect, (c) a simulated Kikuchi pattern supposed on the experimental pattern, and (d) the simulated pattern only for clarity.

Another example of is taken from Figure 2.28(a) on page 23 of Edington's book (1975), which is a complex Kikuchi pattern of the Mg sample. The simulated patterns were carried out separately along all three Kikuchi poles, which shows how the zone axes and Kikuchi line pairs match the experimental pattern, as shown in Figure 13. In the calculation, the high tension of the microscope is assumed to be 100 kV, and the crystal structure of Mg phase, hcp, $P6_3/mmc$, $a =$ 3.1094 Å and $c =$ 5.2108 Å is used.
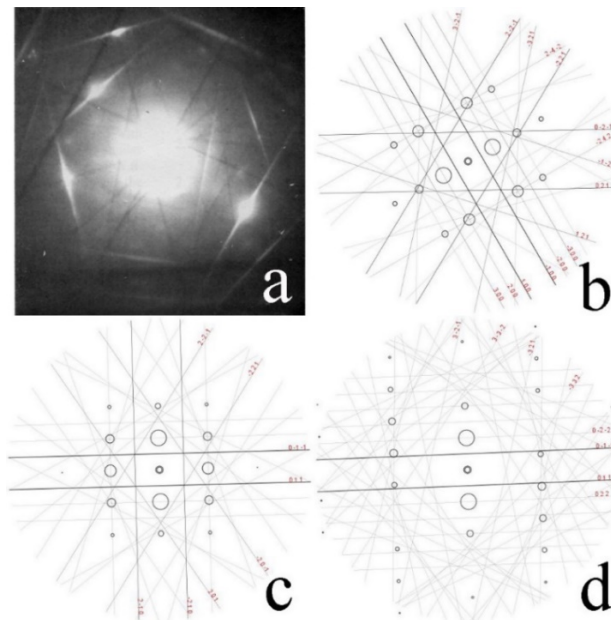

Figure 13. (a) A complex experimental pattern of Mg in Edington's book. (b-d) Three simulated Kikuchi patterns along the zone axes of [0 -1 2], [-1 -2 2], and [1 3 -3].
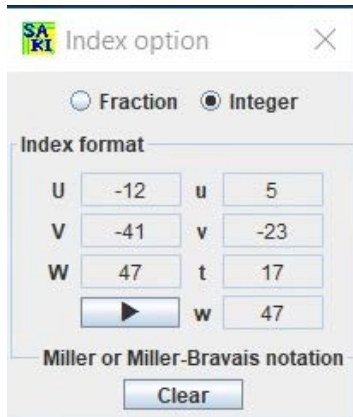
Figure 14. The option for fractional and integer indices and converting Miller indices to Miller-Bravais indices.

5.2 Precise orientation determination from three Kikuchi bands

The analysis of the Kikuchi pattern for Mg taken from Edington's book (1975) is shown in Figure 6 with the parameters and results. The results are listed in Table 2 for a comparison of SAKI. Figure 14 shows the fractional and integer index options and converting Miller indices to Miller-Bravais indices for the hexagonal system. Due to the accuracy in measurement of the Kikuchi pairs in Edington's book and SAKI, the results are slightly different
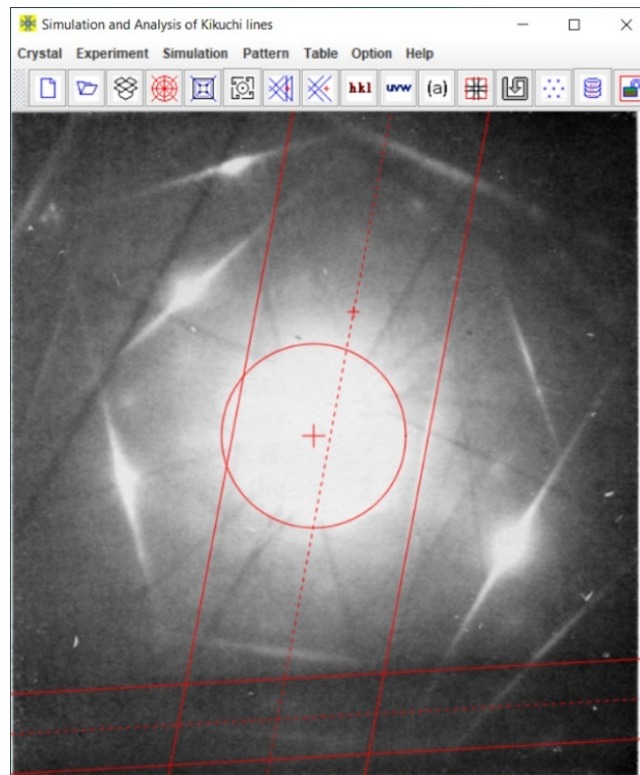

Figure 15. The main panel of SAKI5 features an experimental Kikuchi diffraction pattern. The position of the incident beam has been defined, along with the positions, widths, and directions of two independent pairs of Kikuchi lines.
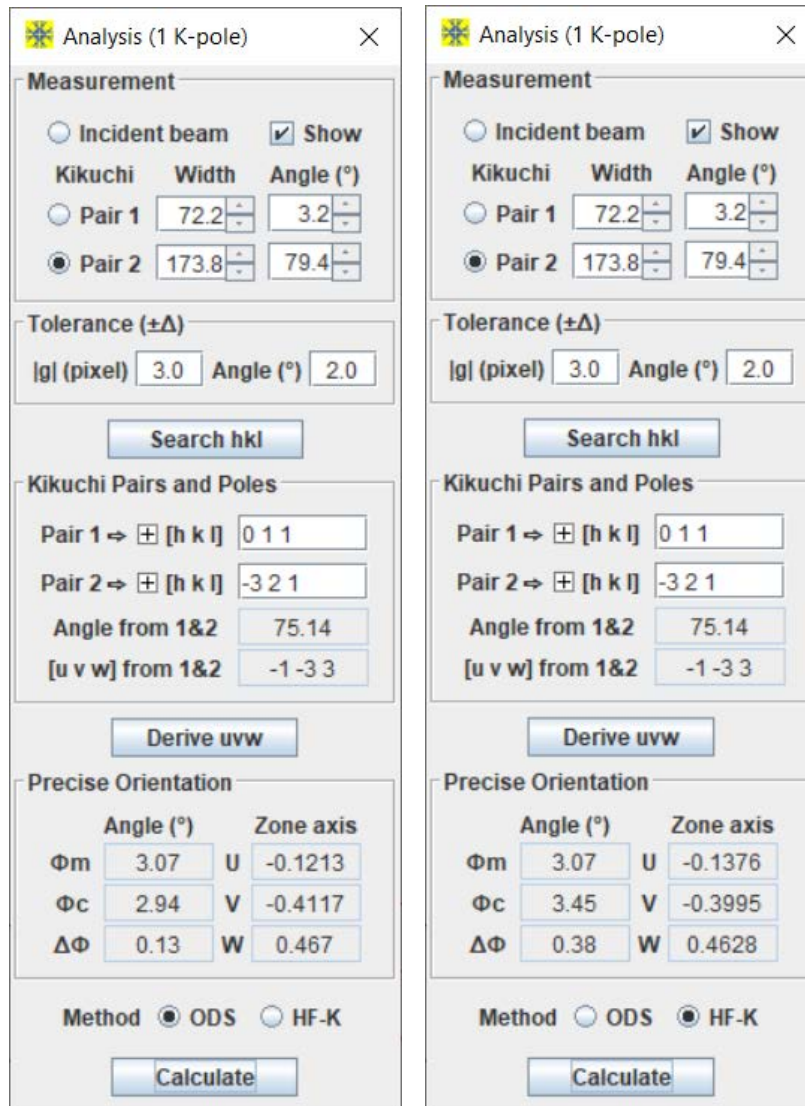
Figure 16. Operational dialog box within SAKI5 for measuring Kikuchi pattern and precisely determining crystal orientation. The applications of (a) the ODS method and (b) the HF-K method.

Table 2. Results from Edington's book and SAKI

Analysis	Φ_1	Φ_2	Φ_3	[u v t w]
Edington's book	3.1°	11.1°	6.5°	[1, -6.024, 5.04, 13.98]
SAKI (measured values)	3.17°	10.37°	6.51°	See the next two rows.
SAKI (analytical method)	3.11°	10.36°	6.48°	[-0.1211, -0.4099, 0.4690]
SAKI (vector method)	3.15°	10.32°	6.57°	[-0.1197, -0.4104, 0.4699]

5.3 Precise orientation determination from two Kikuchi bands

The determination of crystal orientation was also done with both the ODS method and the HF-K method. Figure 15 depicts the main graphical interface of the SAKI5, including an experimental diffraction pattern. Figure 16 showcases the analysis dialog box, featuring options for (a) the

ODS method and (b) the HF-K method. The results are displayed in the lower part of the dialog box in Figure 16. The calculated angles are also listed alongside their corresponding measured angles. As shown in Table 3, the results from both methods are consistent with the previous outcomes obtained using three Kikuchi line pairs (or three Kikuchi poles), thereby affirming the practical utility of these two methods.

Due to measurement errors associated with the positions of the incident beam and Kikuchi line pairs in each measurement, there exists a slight angular discrepancy between the incident beam and the Kikuchi pole in both measurements. Comparing the two methods, the angle calculated by the ODS method (2.94°) is slightly smaller than the measured angle (3.07°). The angle calculated by the HF-K method (3.45°) is slightly larger than the measured angle (3.07°). However, when averaging the zone axes [UVW] obtained from both methods, the calculated angle (3.11°) is very close to the measured angle (3.07°), as shown in Table 3.

Table 3. The results of the two methods and the averaged values

Method	U	V	W	Φ_c (°)	$\Delta\Phi$ (°)
ODS	-0.1213	-0.4117	0.467	2.94	0.13
HF-K	-0.1376	-0.3995	0.4628	3.45	0.38
Average	-0.1295	-0.4056	0.4649	3.11	0.04

6. Related components in Landyne suite

All software components in the Landyne suite use the input structure data in the same format. A selection of them is listed here, which can be used in combination with the SAKI. Users may check the program specification or user's manual for each program in detail.

6.1 SVAT software

SVAT [2020b] is a structural viewer and an analytical tool that uses the same input data format in the Landyne suite and users.

6.2 SAED software

SAED [Li, 2019] can simulate spot patterns from multiple crystal files for comparison or for the simulation of various twins and coexisting structures with a fixed orientation. SAKI is used to analyze precise orientation, and SAED is used for the determination of the zone axis. SAKI and SAED can be viewed as an extension of each other.

6.3 SPICA software

SPICA [Li, 2016] is designed for stereographic projection with an application for specimen orientation adjustment using TEM holders. SPICA can be used to generate a Kikuchi map.

References

Edington, J. W., Practical Electron Microscopy in Materials Science, Monograph Two: Electron Diffraction in the Electron Microscope. Philips, 1975.

Helfmeier H. and Feller-Kniepmeer M., Analytical Determination of the Exact Primary Beam Direction from Kikuchi Patterns. J. Appl. Phys. 48 (1977) 3997.

Jin, Y.L., Li, X.Z. and Sellmyer, D.J., A new tetragonal phase in CoFeCrGe Heusler alloy, Mater. Charter. 136 (2018) 302-309.

Kuo, K.H., Ye, H.Q. and Wu, Y.K., Application of Electron Diffraction Pattern in Crystallography (in Chinese), Science Press, Beijing, 1983.

Li. X.Z., SPICA - Stereographic Projection for Interactive Crystallographic Analysis. J. Appl. Cryst. 49 (2016) 1818-1826.

Li. X.Z., On precise determination of crystal orientation with Kikuchi pattern, Journal of Materials Education, 42:1-2 (2020a) 97-104.

Li. X.Z., SVAT4 – a computer program for crystal structure visualization and analysis
J. Appl. Cryst. 53(2020b) 848-853.

Li. X.Z., SAED3: simulation and analysis of electron diffraction patterns. Microscopy and Analysis, May issue (2019) 16-19.

Liu, W.X., Huang, X.Y. and Chen, Y.R., Electron Microscopy Analysis on Material Structures (in Chinese), Tianjin University press, 1989.

Otte, H.M., Dash, J. and Schaak, H.F., Electron Microscopy and Diffraction of Thin Films : Interpretation and Correlation of Images and Diffraction Patterns. Phys. Stat. Sol. 5 (1964) 527-549.

Thomas, G. and Goringe, M.J., Transmission Electron Microscopy of Materials, John Wiley & Sons, 1979.